JJMIE

Volume 9 Number 2, April.2015
ISSN 1995-6665
Pages 85 - 102

Jordan Journal of Mechanical and Industrial Engineering

Hybrid DEBBO Algorithm for Tuning the Parameters of PID Controller Applied to Vehicle Active Suspension System

Kalaivani Rajagopal * [a], Lakshmi Ponnusamy[b]

[a]Research Scholar, DEEE, CEG, Anna University, Chennai, India
[b] Professor, DEEE, CEG, Anna University, Chennai, India

Received 6 Nov 2014 Accepted 9 May 2015

Abstract

This paper highlights the use of hybridizing Biogeography-Based Optimization (BBO) with Differential Evolution (DE) algorithm for parameter tuning of Proportional Integral Derivative (PID) controller applied to Vehicle Active Suspension System (VASS). Initially BBO, an escalating nature enthused global optimization procedure based on the study of the ecological distribution of biological organisms, and the hybridized DEBBO algorithm which inherits the behaviours of BBO and DE, were used to find the tuning parameters of the PID controller to improve the performance of VASS. Simulations of passive system, active system, having PID controller with and without optimizations, were performed by considering trapezoidal, step and a random kind of road disturbances in MATLAB/SIMULINK environment. The simulation results point out an improvement in the results with the DEBBO algorithm which converges faster than BBO..

Keywords: *Vehicle Active Suspension, Biogeography-Based Optimization (BBO), Differential Evolution (DE), DEBBO, Simulation*.

1. Introduction

The vibration of the vehicle body can cause an unwanted noise in the vehicle, a damage to the fittings attached to the car and severe health problems, such as an increase in the heart rate, spinal problems, etc. to the passengers. Research and the development sections of automobile industries hence promote research on vibration control. For vehicle handling and ride comfort, the suspension system of an automobile plays an essential role. Vehicle handling depends on the force acting between the road surface and the wheels. The ride comfort is related to vehicle motion sensed by the passenger. To improve vehicle handling and the ride comfort performance, in preference to conventional passive system, semi-active and active systems are being developed. The passive system uses a static spring and a damper where as a semi-active suspension involves the use of dampers with variable gain. On the other hand, an active suspension involves the passive components augmented by actuators that supply additional forces and possesses the ability to reduce the acceleration of sprung mass continuously as well as to minimize the suspension deflection which results in the improvement of the tyre grip with the road surface [1; 2].

Research on the control strategies of Vehicle Active Suspension System (*VASS*) has been concentrated on by academicians as well since this problem is open to all. In the past, many researchers explored several control approaches hypothetically, simulated them with simulation software, confirmed practically and proposed for the control of active suspension system. The survey of optimal control technique applications to the design of active suspensions are listed in [3] and the emphasis is on Linear-Quadratic (*LQ*) optimal control. A method for designing a controller with a model which includes the passenger dynamics is presented in [4]. The comparison of Linear Matrix Inequality (*LMI*) based controller and optimal Proportional Integral Derivative (*PID*) controller by Abdalla *et al.* [5] proved the sprung mass displacement response improvement by *LMI* controller with only the suspension stroke as the feedback.

PID controller design is discussed in [5-7]. The design of robust *PI* controller which is used to obtain an optimal control is discussed in [8]. The conclusion, made by Dan Simon [9], stimulated the idea of using Biogeography-Based Optimization (*BBO*) for the optimization of *PID* parameters.

In [10] the classification of the satellite image of a particular land cover using the theory of *BBO* is highlighted, concluding that with this, highly accurate land cover features can be extracted effectively. To optimize the element length and spacing for Yagi-Uda antenna, *BBO* is used and the performance is evaluated with a method of moment's code NEC2 [11]. *BBO* algorithm, to solve both convex and non-convex Economic Load Dispatch (*ELD*) problems of thermal plants, is proposed and suggested as a

* Corresponding author. e-mail: kalaivanisudhagar@gmail.com.

promising alternative approach for solving the *ELD* problems in practical power system [12]. Markov theory for partial immigration based *BBO* [13] is used to derive a dynamic system model. A better insight into the dynamics of migration in actual biogeography systems is given [14]; it also helped in understanding the search mechanism of *BBO* on multimodal fitness landscapes. In [15], a multi-objective *BBO* algorithm is proposed to design optimal placement of phasor measurement units, which makes the power system network completely observable and the simultaneous optimization of the two conflicting objectives, such as minimization and maximization of two different parameters, are performed. The effectiveness of *BBO* over Genetic Algorithm (*GA*) and Particle Swam Optimization (*PSO*) is highlighted [16] for an *ELD* problem. The performance of *BBO* is tested for real-world optimization problems with some benchmark functions [17]. An improved accuracy yielding algorithm is presented [18], in which the performance of *BBO* is accelerated with the help of a modified mutation and clear duplicate operators; the suitability of *BBO* for real time applications is also discussed. A combination of Differential Evolution (*DE*) and *BBO* is designed to accelerate the convergence speed of the algorithm and of improving the solution for the economic emission load dispatch problem [19].

In the present paper, the preference is to optimize the *PID* controller tuning parameters with hybridized *DEBBO* to improve the rapidity of convergence. The likelihood of the proposed method was verified in terms of the computational efficiency and the outputs of the linear *VASS* models which are considered for the simulation study in comparison with *BBO*.

The present study is organized as follows: Quarter Car (*QC*) model and Half Car (*HC*) model dynamics of an active suspension system are briefly explained in section 2. Discussion of the control scheme is presented in section 3. In section 4, the simulation results are presented and discussed. The final section presents the conclusion of the study.

2. Active Suspension System

The passive suspension system has the ability to only store and dissipate energy. Its parameters, such as spring stiffness and damping coefficients, are fixed in order to achieve a certain level of compromise between road holding, load carrying and comfort. The semi active suspension system involves a variable damper, while the active suspension system has the ability to store, dissipate and introduce energy to the system; it may vary its parameters depending on the working conditions.

2.1. Quarter Car Model

A two-Degree of Freedom (*DOF*) *QC* model of *VASS* is shown in Figure 1. It represents the automotive system at each wheel, i.e., the motion of the axle and the vehicle body at any one of the four wheels of the vehicle. The *QC* model, used in [20], is considered because it is simple and one can observe the basic features of the *VASS* such as sprung mass displacement, body acceleration, suspension deflection and tyre deflection. The suspension model consists of a spring k_s, a damper c_s and an actuator of active force F_a. For a passive suspension, F_a can be set to zero. The sprung mass m_s represents the *QC* equivalent of the vehicle body mass. An unsprung mass m_u represents the equivalent mass due to axle and tyre. The vertical stiffness of the tyre is represented by the spring k_t. The variables y_s, y_u and y_t represents the vertical displacements from static equilibrium of sprung mass, unsprung mass and the road, respectively. Equations of motion of the two *DOF QC* model of *VASS* are given in (1). It is assumed that the suspension spring stiffness and tyre stiffness are linear in their operating ranges and that the tyre does not leave the ground. The state space representation (2) of *QC* model is given below:

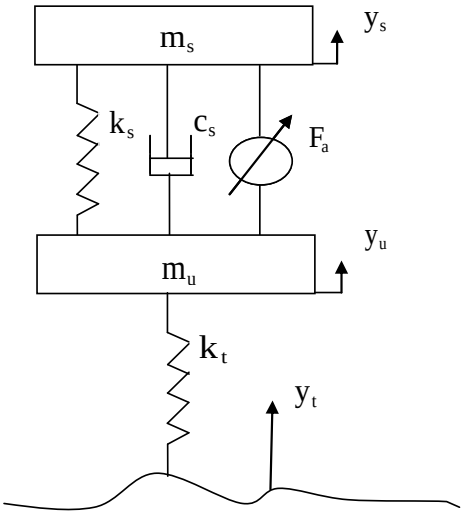

Figure 1. Quarter Car model

$$m_s \ddot{y}_s + c_s (\dot{y}_s - \dot{y}_u) + k_s (y_s - y_u) = F_a \quad (1)$$

2.2. Half Car Model

An *HC* active suspension model with 4 *DOF* [21], which represents the combination of two *QC* models, i.e., one front wheel, one rear wheel and the associated axle parts of a car (Figure 2), was taken. It includes sprung mass m_s, front unsprung mass m_{uf}, rear unsprung mass m_{ur}, front suspension damping coefficient c_{sf}, rear suspension damping coefficient c_{sr}, front suspension stiffness k_{sf}, rear suspension stiffness k_{sr}, front tyre damping coefficient c_{tf}, rear tyre damping coefficient c_{tr}, front tyre stiffness k_{tf}, rear tyre stiffness k_{tr}, pitch moment of inertia I_p, distance of front axle to sprung mass Center of Gravity (*CG*) L_f, distance of rear axle to sprung mass *CG* L_r, front actuator force F_{af} and

the rear actuator force F_{ar}. y_s, θ are the vertical displacement and the pitch angle of the sprung mass at the *CG*, y_{sf}, y_{sr} are the vertical displacement of front and rear suspensions, y_{uf}, y_{ur} are the unsprung mass displacements and y_{tf}, y_{tr} are the tyre displacements at the front and rear. It is assumed that the *HC* model system is linear, the tires always have contact with the road and the forces due to moment and backlash in various joints, linkages and gear are neglected.

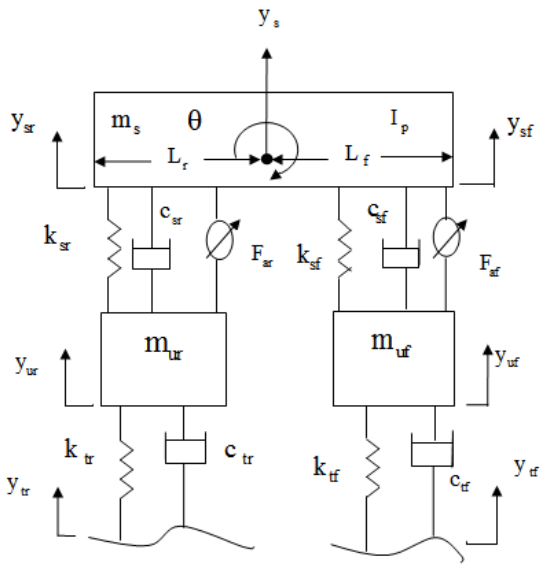

Figure 2. Half Car model

$$m_u \ddot{y}_u - c_s(\dot{y}_s - \dot{y}_u) - k_s(y_s - y_u) - k_t(y_t - y_u) = -F_a \tag{2}$$

$$\ddot{y}_{ur} = \frac{[-k_{tr}(y_{ur} - y_{tr}) - c_{sr}(\dot{y}_{ur} - \dot{y}_{sr}) - k_{sr}(y_{ur} - y_{sr}) - c_{tr}(\dot{y}_{ur} - \dot{y}_{tr}) - F_{ar}]}{m_{ur}} \tag{3}$$

$$\ddot{y}_{uf} = \frac{[-k_{tf}(y_{uf} - y_{tf}) - c_{sf}(\dot{y}_{uf} - \dot{y}_{sf}) - k_{sf}(y_{uf} - y_{sf}) - c_{tf}(\dot{y}_{uf} - \dot{y}_{tf}) - F_{af}]}{m_{uf}} \tag{4}$$

$$\ddot{y}_s = \frac{-[k_{sr}(y_{sr} - y_{ur}) + k_{sf}(y_{sf} - y_{uf}) + c_{sr}(\dot{y}_{sr} - \dot{y}_{ur}) + c_{sf}(\dot{y}_{sf} - \dot{y}_{uf}) - F_{ar} - F_{af}]}{m_s} \tag{5}$$

$$\ddot{\theta} = \frac{-L_r[(c_{sr}(\dot{y}_{sr} - \dot{y}_{ur}) + k_{sr}(y_{sr} - y_{ur})] + L_f[k_{sf}(y_{sf} - y_{uf}) + c_{sf}(\dot{y}_{sf} - \dot{y}_{uf})] - L_f F_{af} + L_r F_{ar}}{I_s} \tag{6}$$

$$y_{sr} = y_s - L_r\theta \tag{7}$$

$$y_{sf} = y_s + L_f\theta \tag{8}$$

For the passive suspension system, the control forces in the front and rear F_{af} and F_{ar} are equal to 0.

3. Controller Design

3.1. PID Controller

Most of the automated industrial processes include a *PID* controller which is a combination of proportional, integral and derivative controller that can improve both the transient and the steady state performance of the system. The mathematical representation of the simple *PID* control scheme is given by:

$$G_c = k_p e(t) + k_i \int e(t)dt + k_d \frac{de}{dt} \tag{9}$$

where G_c is the controller output

k_p proportional gain

k_i integral gain

k_d differential gain

$e(t)$ input to the controller

$\int e(t)dt$ time integral of the input signal

$\frac{de}{dt}$ time derivative of the input signal

To reduce the effect of the road disturbance input (Figure 3), two suspension parameters, suspension deflection ($y_S - y_U$) and velocity, are feedback to the controllers [20]. The feedback gains are G_e and G_V, respectively. The output control signals are amplified by a gain G_U and, then, given as the input to the actuator. In the present work, the nonlinear dynamics of actuator are not considered and the gain of the linear actuator is taken as G_a. The actuator force F_a, which is the additional input to the system, is proportional to the controller output to have better comfort. An autotuning for both PID_1 and PID_2 was carried out using a robust response tuning metod with the MATLAB simulation software.

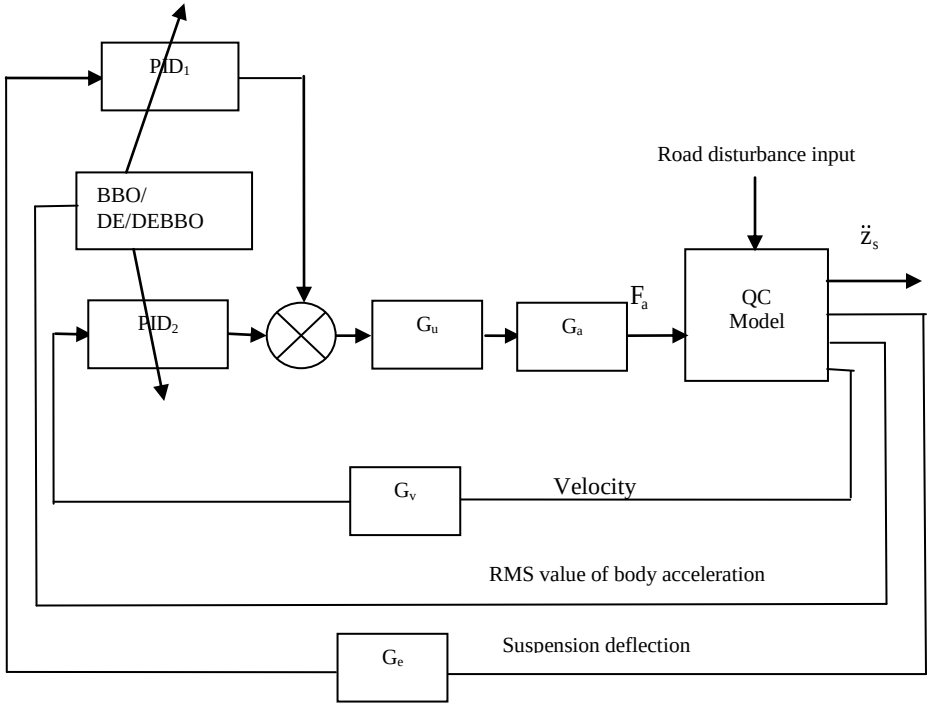

Figure 3. The block diagram representation of control scheme of VASS using PID controller

3.2. Optimization of PID Controller

In the present work, *BBO*, *DE* and *DEBBO* techniques are used to find the *PID* tuning parameters, such as k_p, k_i and k_d, of both the controllers PID_1 and PID_2 (Figure 3) to give an optimum [22] *RMS* value of body acceleration. To optimize the continuous time body acceleration signal (*f(t)*) energy, the cumulative *RMS* value is taken; it is given as follows:

$$J = \sqrt{\frac{1}{T}\int_0^T \|f(t)\|^2 \, dt} \tag{10}$$

where *T* is the vibration period in seconds.

3.2.1. Biogeography Based Optimization Based PID Controller

A population based *BBO* technique was developed based on the theory of Biogeography [9] which describes how species voyage from one habitat to another, how new species come up and species become vanished. A habitat is a geographically isolated island from other habitats. Each habitat has its individual features which are specified by the Habitat Suitability Index (*HSI*) variables. A habitat with high *HSI* is well suited for species living. The migration of a species among habitats takes place when the high *HSI* habitats have more species or when a habitat has low *HSI*. This process is known as emigration. Another process called immigration and takes place when the species move towards the habitat with high *HSI* having few species. The emigration and immigration of species from a habitat are called migration. The emigration rate (μ) and immigration rate (λ) vary with the number of species available in the habitat. With no species, the immigration rate touches the upper limit and with the maximum number of species, it is zero, whereas the emigration rate increases with the increase in the number of species. The change in *HSI* due to a natural disaster is taken into account with the mutation operation.

The optimization steps of *BBO* algorithm [15] are described as follows:

1. Initialize the optimization problem, the *BBO* parameters and the habitats.
2. Perform *BBO* operations such as migration and mutation.
3. Modify the habitats.
4. Check the stopping criteria; if not achieved, repeat from step 2.

BBO does not involve the reproduction of a solution as in *GA*. In each generation, the fitness of every solution (habitat) is used to find the migration rates.

For the *BBO* based *PID* (*BBOPID*) controller [23], the following parameters are initialized: population size, the maximum species count (S_{max}), maximum emigration rate (E), maximum immigration rate (I), maximum mutation rate (m_{max}), habitat modification probability (P_{mod}), number of decision variables, the number of habitats, maximum number of generations, mutation probability, and migration probability.

1. The individual habitat variables are random initialized.
2. Mapping of *HSI* to the number of species S, calculation of the emigration rate and immigration rate using equations 11 and 12 are performed.

$$\lambda = I(1 - \frac{d}{S_{max}}) \tag{11}$$

$$\mu = \frac{E \times d}{S_{max}} \tag{12}$$

where d is the number of species at the instant of time.

3. The BBO operation migration is performed based on the definition 7 in [9] and the HSI is recomputed.
4. Then the mutation operation is performed as in definition 8 in [9] and the HSI is recomputed. The emigration and immigration rates of each solution are useful in probabilistically sharing the information between the habitats. Each solution can be modified with the habitat modification probability Pmod to yield good solution.
5. From step 2 the computation is repeated for the next iteration. The loop is terminated after predefined number of generations or after achievement of acceptable solution.

Parameter Initialization for *BBO*		
Modification probability		= 1
Mutation probability		= 0.05
Selectiveness parameter	δ	= 2
Max immigration rate		= 1
Max emigration rate		= 1
Step size used for numerical integration		= 1
Lower bound and Upper bound for immigration probability per gene		= [0.01, 1]

3.2.2. Differential Evolution Based PID Controller

Technically, a simple population-based Differential Evolution (*DE*) algorithm [24, 25] having a self-organizing ability, is suitable even for non-linear systems and can be used for a continuous function optimization for tuning of *PID* controller parameters. Basic steps involved in *DE* algorithm are:

1. Initialization
2. Evaluation
3. Repeat

{ Mutation
Recombination
Evaluation
Selection }
Until fitness function is minimized.

Generate the mutant vector $v_{i,G+1}$ (13) for each target vector $x_{i,G}$, $i=1,2,3\ldots\ldots N$ where N is the number of parameter vectors in the population.

$$v_{i,G+1} = x_{r1,G} + F.(x_{r2,G} - x_{r3,G})$$
$$r_1, r_2, r_3 \in \{1, 2, \ldots\ldots N\} \tag{13}$$

The real and constant scaling factor for differential variation $F \in [0,2]$

The trial vector for crossover operation is

$$u_{i,G+1} = (u_{1i,G+1}, u_{2i,G+1} \ldots\ldots u_{Di,G+1}) \tag{14}$$

where

$$u_{ji,G+1} = v_{ji,G+1} \quad if(randb(j) \le CR) or j = rnbr(i)$$
$$x_{ji,G} if(randb(j) > CR) and j \ne rnbr(i) \tag{15}$$
$$j = 1, 2, \ldots\ldots D$$

where

$CR \in [0,1]$ is the crossover constant

$randb(j) \in [0,1]$ is the j^{th} evaluation of uniform random number

$rnbr(i) \in 1, 2, \ldots\ldots D$ randomly chosen index which ensures that $u_{i,G+1}$ gets at least one parameter from $v_{i,G+1}$.

The fitness criterion is used to decide whether the trial vector is a member of next generation. If the fitness value of the trial vector $u_{i,G+1}$ is better than that of target vector $x_{i,G}$, then, in next generation, the target vector $x_{i,G+1}$ is assigned to be $u_{i,G+1}$. Otherwise first generation value $x_{i,G}$ is retained.

Parameter Initialization for *DE*	
Scaling factor	F = 0.5
Crossover constant	CR = 0.5

3.2.3. Hybridization

The *BBO* algorithm, without hybridizing with any evolutionary algorithms, does not have much diversity in local or sub optimal solutions. In *DEBBO*, a hybrid migration operator of *BBO* is applied along with mutation, crossover and selection operators of *DE* which combines the searching of *DE* with the operation of *BBO* effectively to speed up the convergence property [26, 27] and to find better quality results.

Parameters for *DEBBO* are initialized as in *BBO* and *DE*.

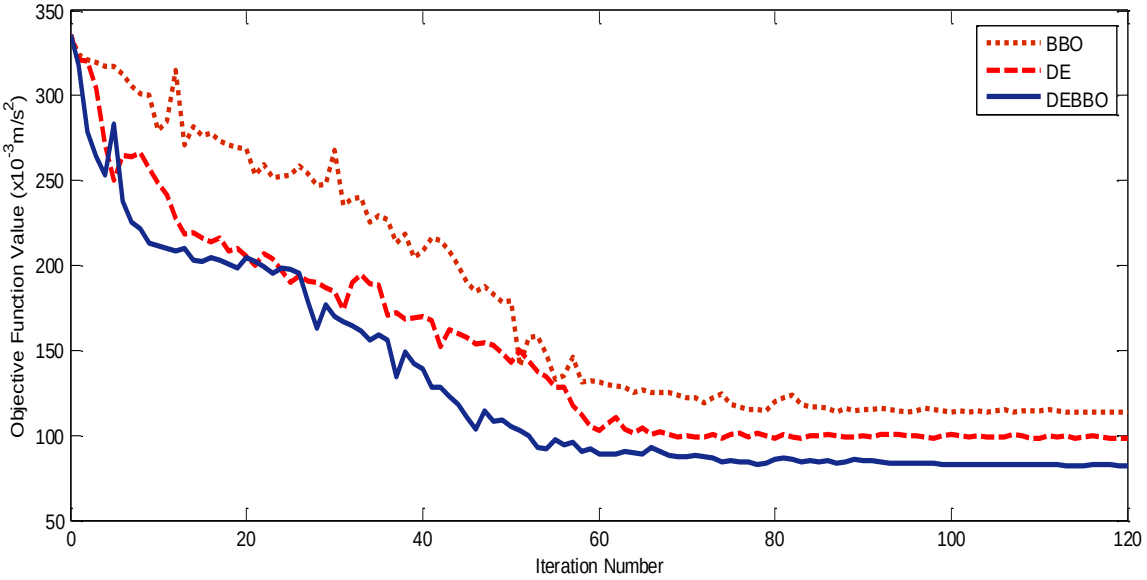

Figure 4. Statistics of search process

The optimization results were computed by averaging 20 minimization runs and the convergence characteristics of each technique are shown in Figure 4. As the convergence rate is fast in the case of *DEBBO*, the corrective actions can be taken quickly compared to the *BBO* without hybridization for a *VASS*. *DEBBO* yields sub linear convergence. Each run yielded the global minimum results. From the convergence plot, *DEBBO* is found to be superior to the *BBO* algorithm.

4. Simulation

The parameters of the *QC* model, taken from [20], are listed below:

Sprung mass (m_s) : 290 kg

Unsprung mass (m_u) : 59 kg

Damper coefficient (c_s) : 1,000 Ns/m

Suspension stiffness (k_s) : 16,812 N/m

Tyre stiffness (k_t) : 190,000 N/m

The parameters of the *HC* model, taken from [21], are listed below:

Sprung mass (m_s) : 430 kg

Pitch moment of inertia (I_p) : 600 kgm^2

Front unsprung mass (m_{uf}) : 30 kg

Rear unsprung mass (m_{ur}) : 25 kg

Front suspension damping coefficient (c_{sf}) : 500Ns/m

Rear suspension damping coefficient (c_{sr}) : 400Ns/m

Front tyre damping coefficient(c_{tf}) : 24Ns/m

Rear tyre damping coefficient (c_{tr}) : 24Ns/m

Front suspension stiffness (k_{sf}) : 6666.67N/m

Rear suspension stiffness (k_{sr}) : 10000N/m

Front tyre stiffness (k_{tf}) : 152N/m

Rear tyre stiffness (k_{tr}) : 152N/m

Distance of front axle to sprung mass *CG* (L_f) : 0.871m

Distance of rear axle to sprung mass *CG* (L_r) : 1.469m

International Organization for Standardization gives the classification of road roughness using Power Spectral Density (*PSD*) values. The present study considered, initially, a trapezoidal road disturbance which represents the reflector paved on the road, secondly, a step input which represents a vehicle coming out of a pothole and, thirdly, a random input. For the *HC* model, front road input y_{tf} and a 0.84 sec time delayed rear road input y_{tr} are considered and are shown in Figure 5.

The mathematical model of the vehicle suspension systems *QC* and *HC* is detailed in section 2 with the controllers discussed in sections 3, in which all are simulated with three road input profiles discussed.

The *PID* tuning parameters obtained with a robust response tuning, *BBO*, *DE* and *DEBBO* with trapezoidal input are listed in Table 1. For the suitability of the designed controller for other kinds of road disturbances, the simulation is carried out with step and random type of road inputs.

Table 1. The Optimized PID tuning parameters with BBO, DE and DEBBO

PID Para-meter	**Controller**			
	PID	**BBOPID**	**DEPID**	**DEBBOPID**
kp_1	0.0106	0.0432	0.3810	0.0350
ki_1	0.4159	0.1934	0.2863	0.4076
kd_1	0.0022	0.0050	0.1182	0.0122
kp_2	0.3801	0.8739	2.3007	1.7680
ki_2	0.5632	0.2846	0.5685	0.2289
kd_2	0.0044	0.0383	0.0242	0.0326

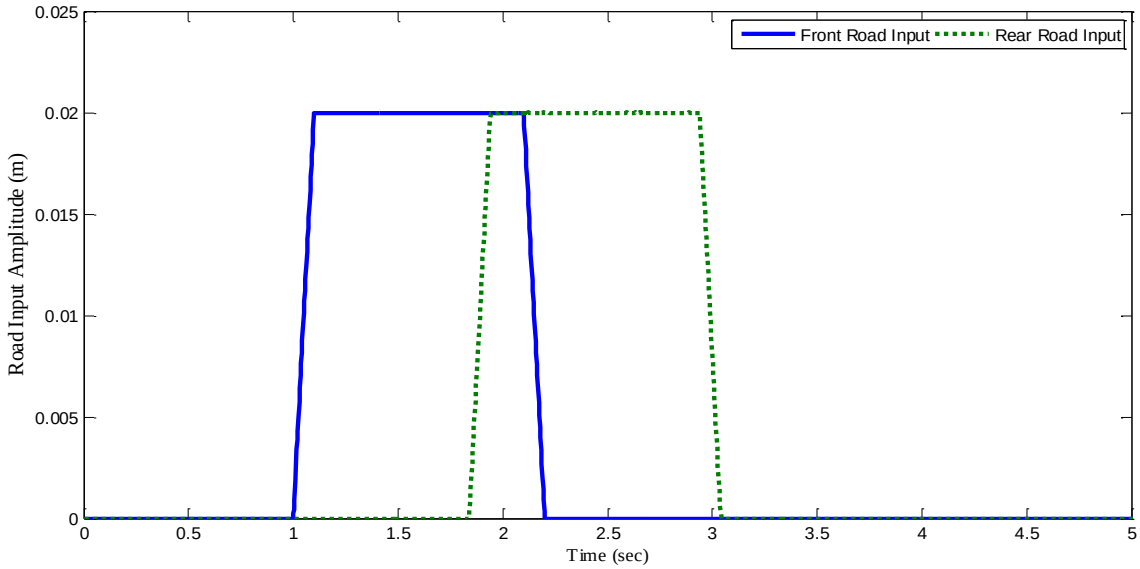

(a)

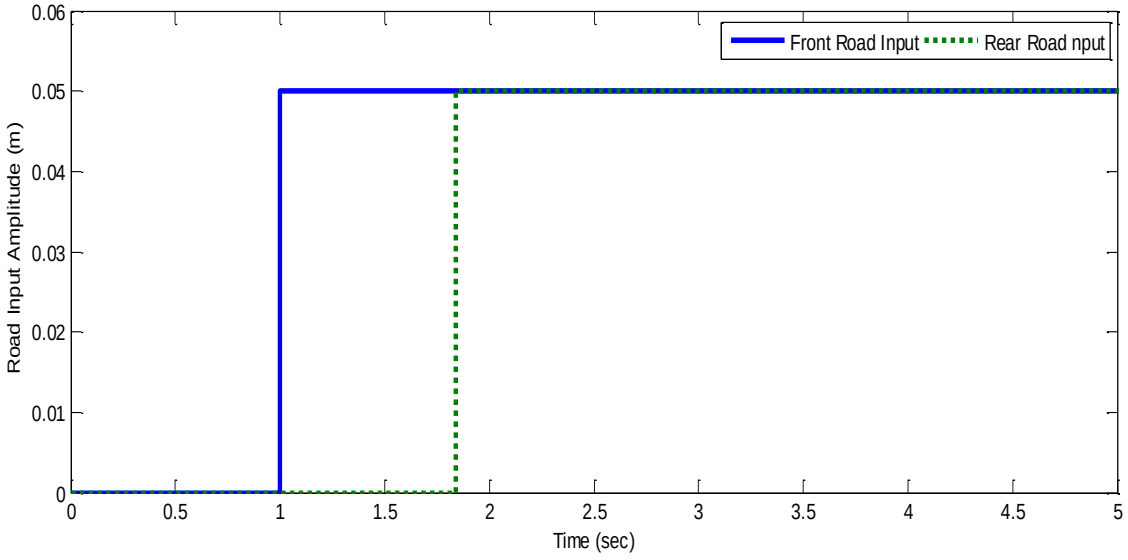

(b)

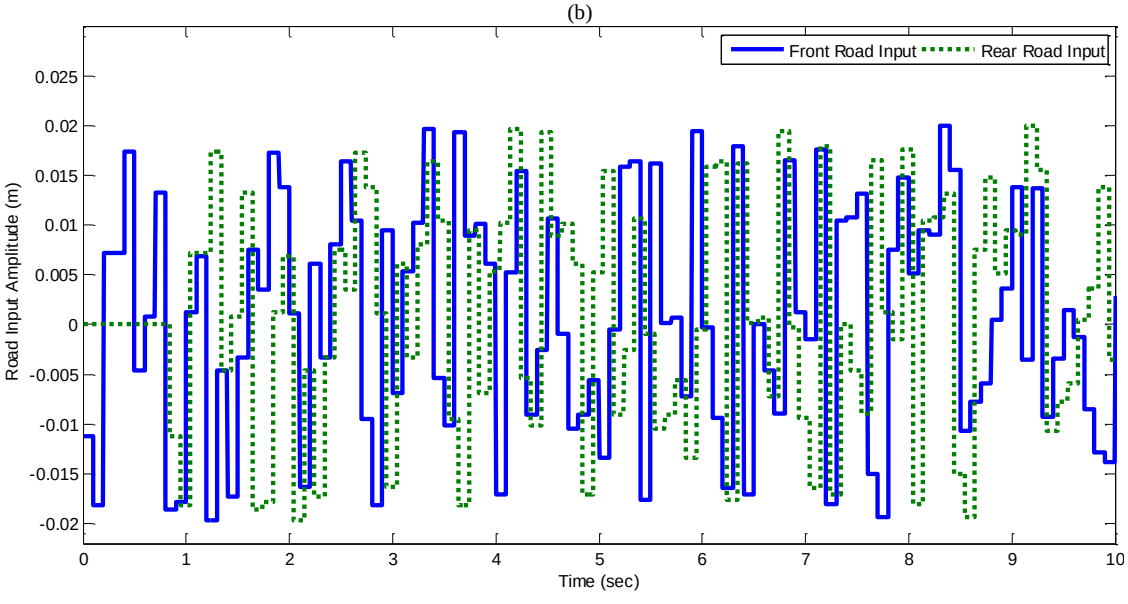

(c)

Figure 5. Road Input profile **:** (a) Trapezoidal Input (b) Step Input (c) Random Input

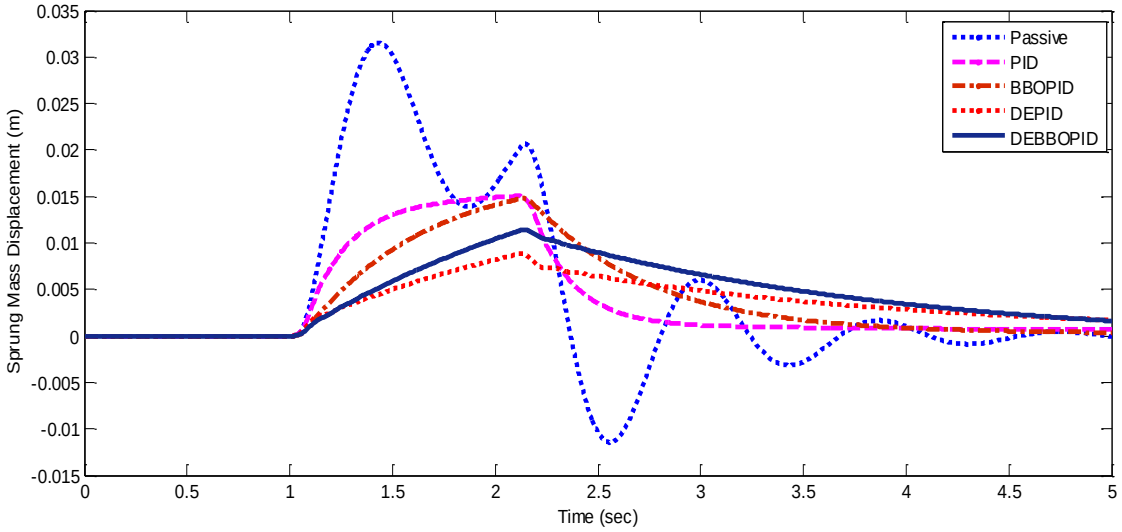

(a)

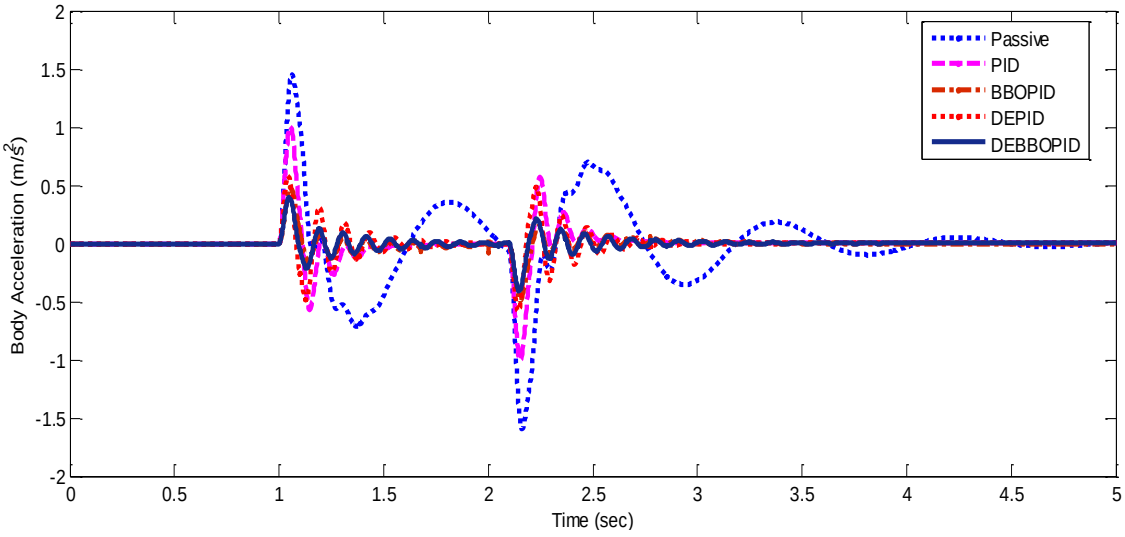

(b)

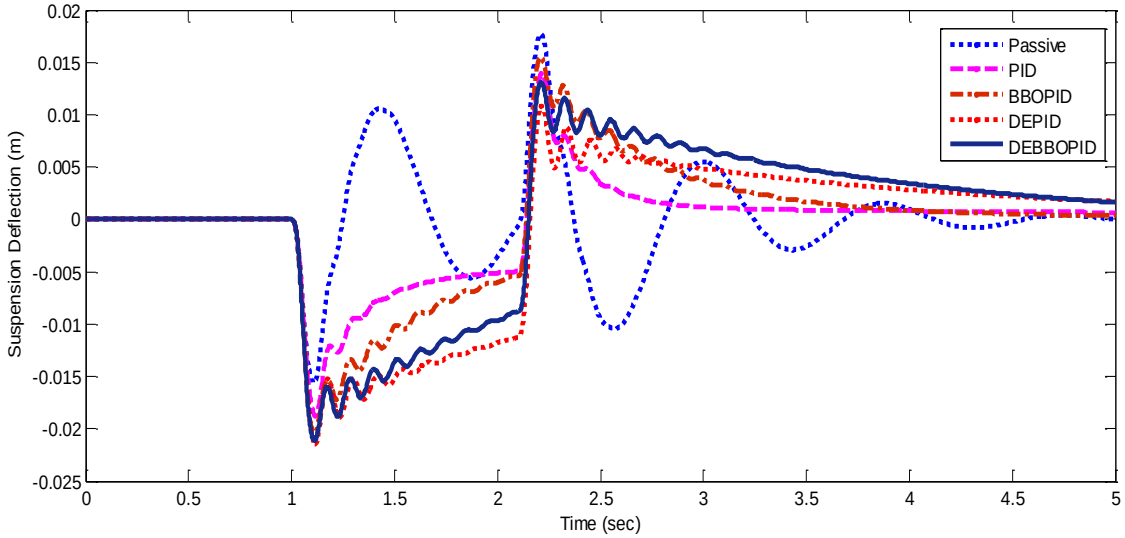

(c)

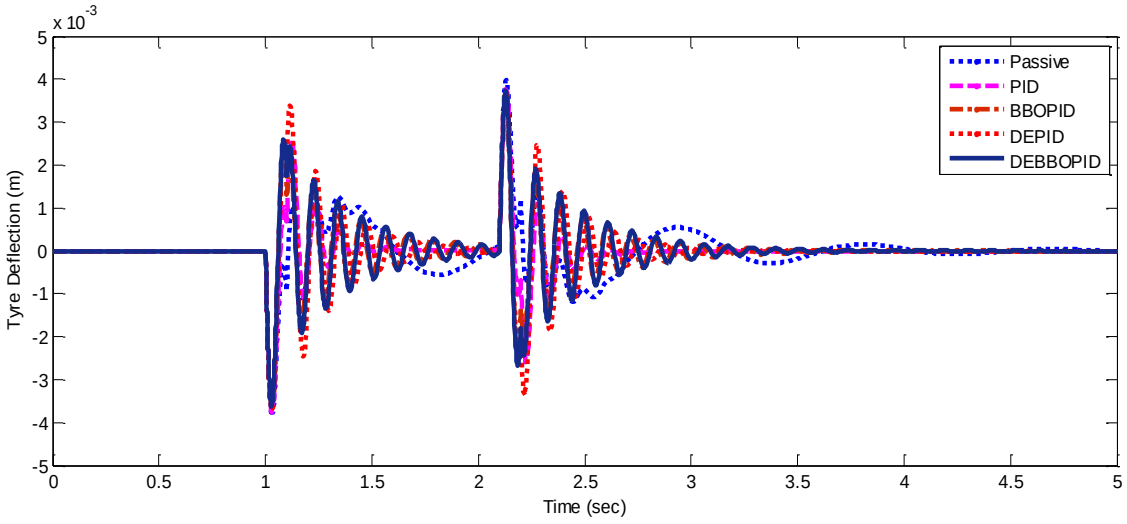

(d)

Figure 6. Time responses of quarter car model with trapezoidal input : (a) Sprung Mass Displacement (b) Body Acceleration (c)Suspension Deflection (d) Tyre Deflection

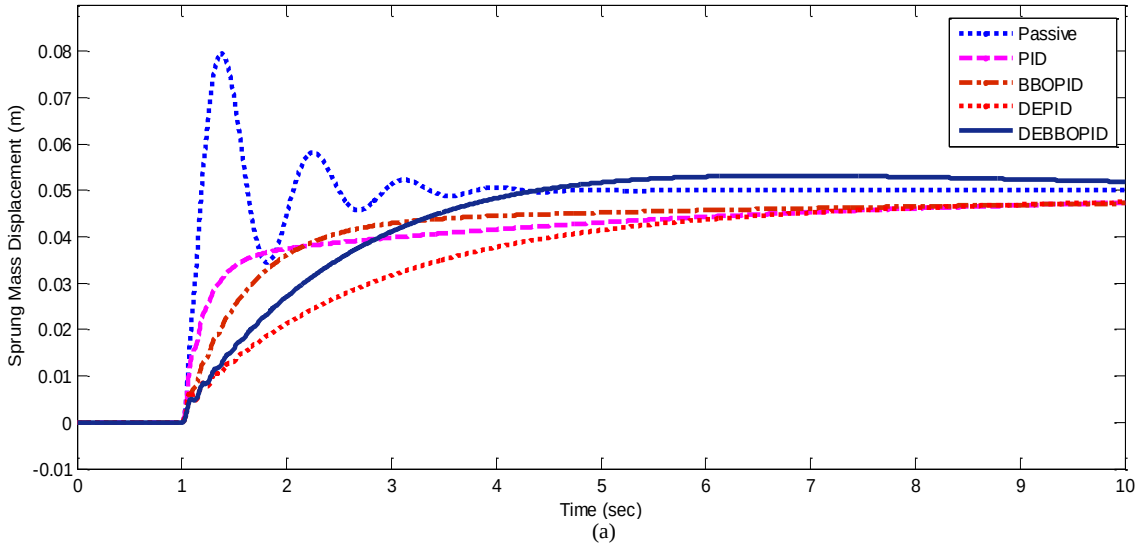

(a)

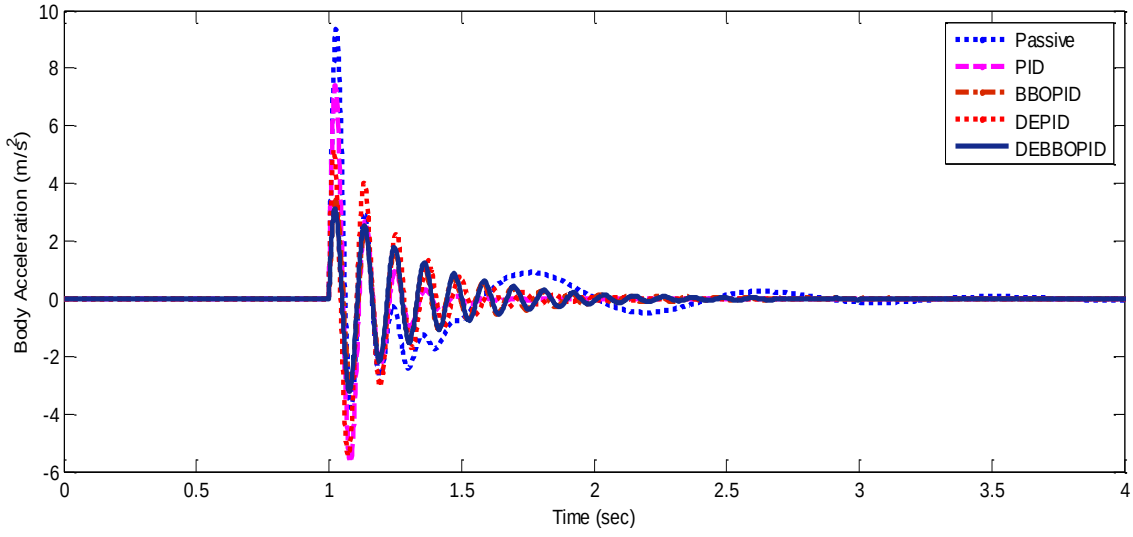

(b)

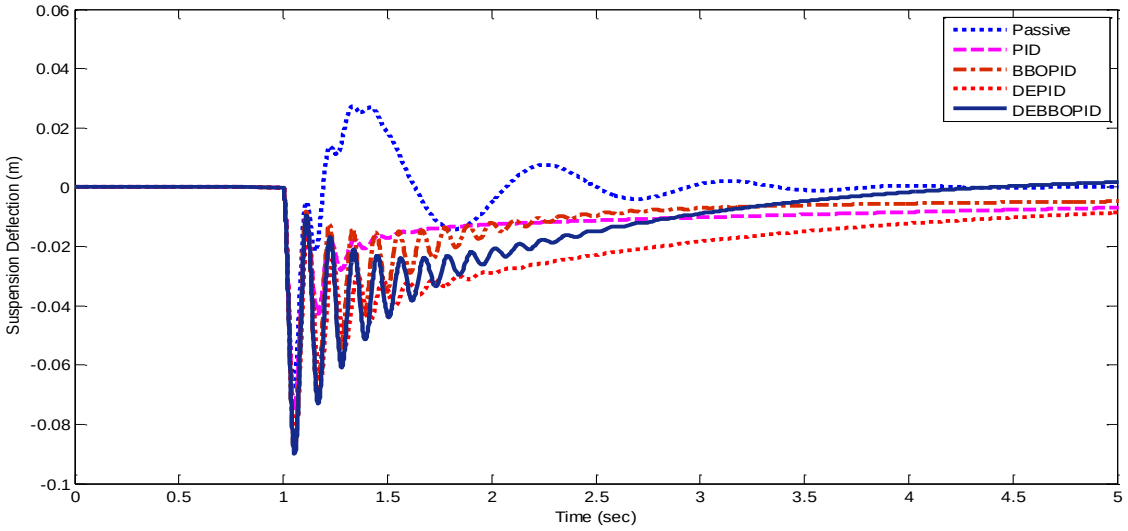

(c)

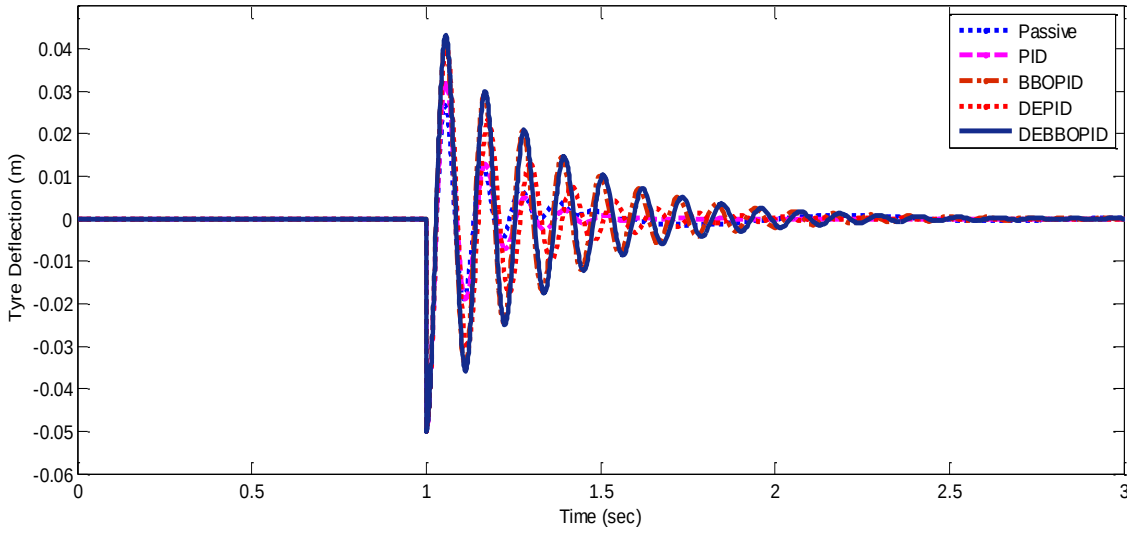

(d)

Figure 7. Time responses of quarter car model with step input : (a) Sprung Mass Displacement (b) Body Acceleration (c) Suspension Deflection (d) Tyre Deflection

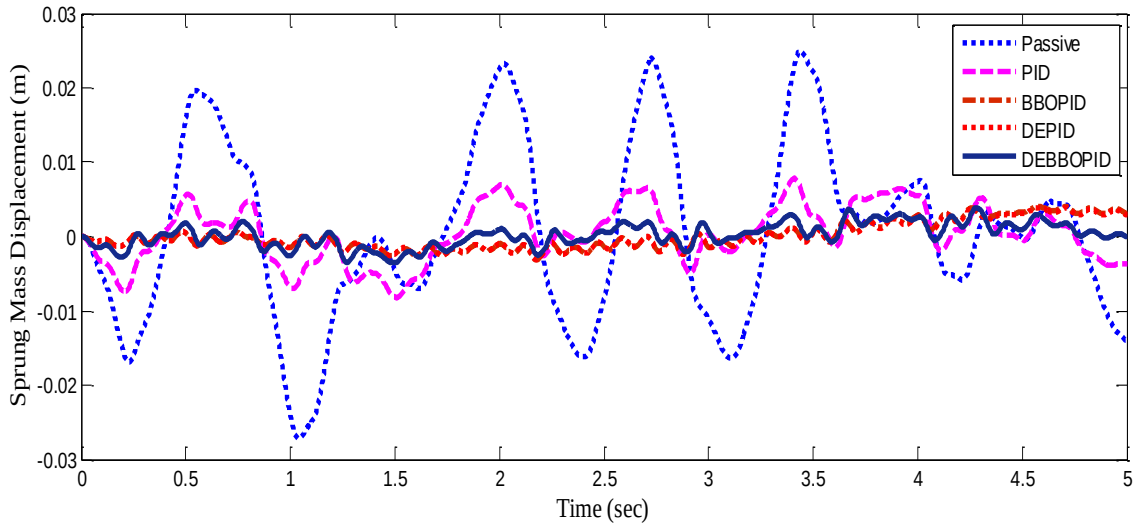

(a)

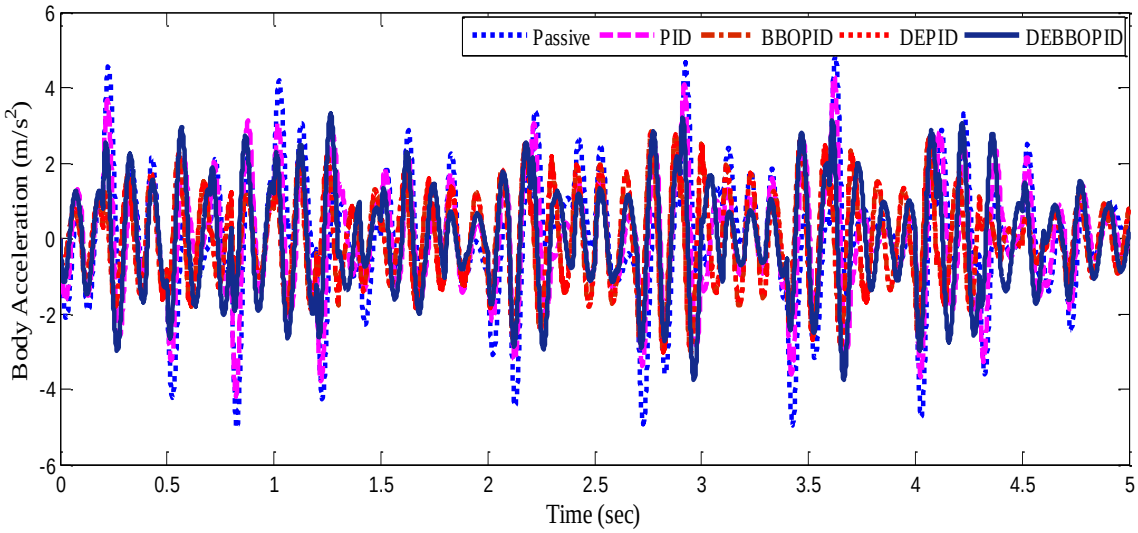

(b)

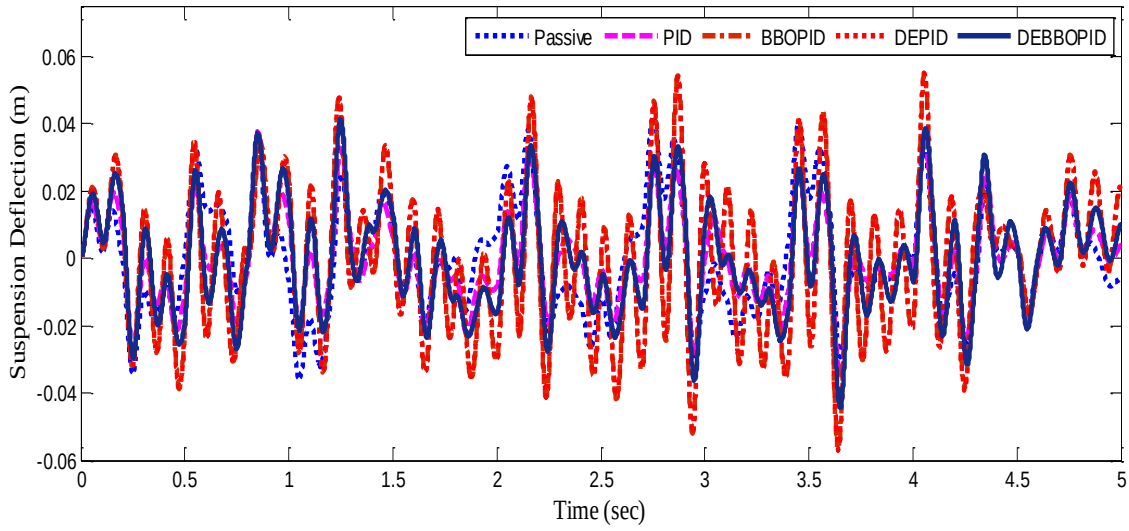

(c)

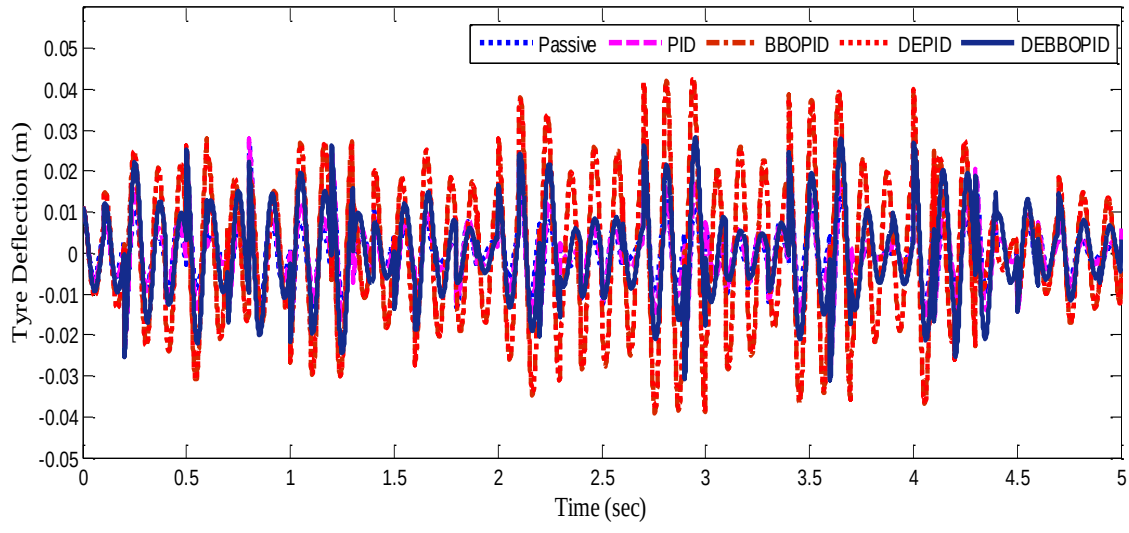

(d)

Figure 8. Time responses of quarter car model with random input : (a) Sprung Mass Displacement (b) Body Acceleration (c) Suspension Deflection (d) Tyre Deflection

The simulation results of *QC* passive system, system with *PID*, *BBOPID*, *DEPID* and *DEBBOPID* controllers are shown in Figures 6, 7 and 8. (a) - (d).

It is clear from Figures 6, 7, 8. (a) and Figures 6, 7, 8. (b) that the sprung mass displacement and vehicle body acceleration is considerably reduced by the proposed *DEBBOPID* controller. It guarantees the travelling comfort to the passengers. Also Figure 6, 7, 8. (c) shows that the suspension deflection with all the controllers are almost the same. Figures 6, 7, 8. (d) illustrate the road holding ability maintained by all the controllers. The tyre displacement of active systems is higher than that of the passive suspension system.

The *RMS* values of the time responses of the four outputs with the three inputs are listed in Tables 2 to 4. It is clear that the *VASS* using *DEBBOPID* controller is useful for the betterment of the ride and travelling comfort with a reduced body acceleration over *PID* controller, with and without *BBO* or *DE* and the passive system.

In the evaluation of the vehicle ride quality, the *PSD* for the body acceleration as a function of frequency is of a prime interest and is plotted for the passive system and that with *PID*, *BBOPID*, *DEPID* and *DEBBOPID* controller for the three different types of road inputs (Figure 9). It is clear from the *PSD* plot that in the human sensitive frequency range 4-8 Hz, compared to *PID*, *BBOPID* and *DEPID*, *DEBBOPID*, reduces the vertical vibrations to a great extent and improves the comfort of travelling when subjected to trapezoidal road input.

Table 2. RMS values of the time responses of quarter car model with trapezoidal input

System	Sprung Mass Displacement ($x10^{-3}$m)	Body Acceleration ($x10^{-3}m/s^2$)	Suspension Deflection ($x10^{-3}$m)	Tyre Deflection ($x10^{-4}$m)
Passive	10.61	336.6	4.81	6.168
PID	6.375	157.2	4.654	5.551
BBOPID	6.147	113.6	6.369	5.899
DEPID	4.294	98.0	7.574	7.278
DEBBOPID	5.575	82.3	7.741	6.563

Table 3. RMS values of the time responses of quarter car model with step input

System	Sprung Mass Displacement ($x10^{-3}$m)	Body Acceleration ($x10^{-3}m/s^2$)	Suspension Deflection ($x10^{-3}$m)	Tyre Deflection ($x10^{-3}$m)
Passive	47.91	655	6.605	2.693
PID	40.36	531.9	9.842	2.903
BBOPID	41.11	526.8	11.32	4.432
DEPID	37.45	501.9	15.95	3.902
DEBBOPID	44.68	260.4	13.31	4.56

Table 4. RMS values of the time responses of quarter car model with random input

System	Sprung Mass Displacement ($x10^{-3}$m)	Body Acceleration ($x10^{-3}m/s^2$)	Suspension Deflection ($x10^{-3}$m)	Tyre Deflection ($x10^{-3}$m)
Passive	28.43	2338.12	194.4	138.89
PID	21.94	1947.34	199.22	179.32
BBOPID	20.13	1802.53	201.5	193.04
DEPID	22.24	1732.521	203.45	200.13
DEBBOPID	21.35	1581.09	205.39	208.96

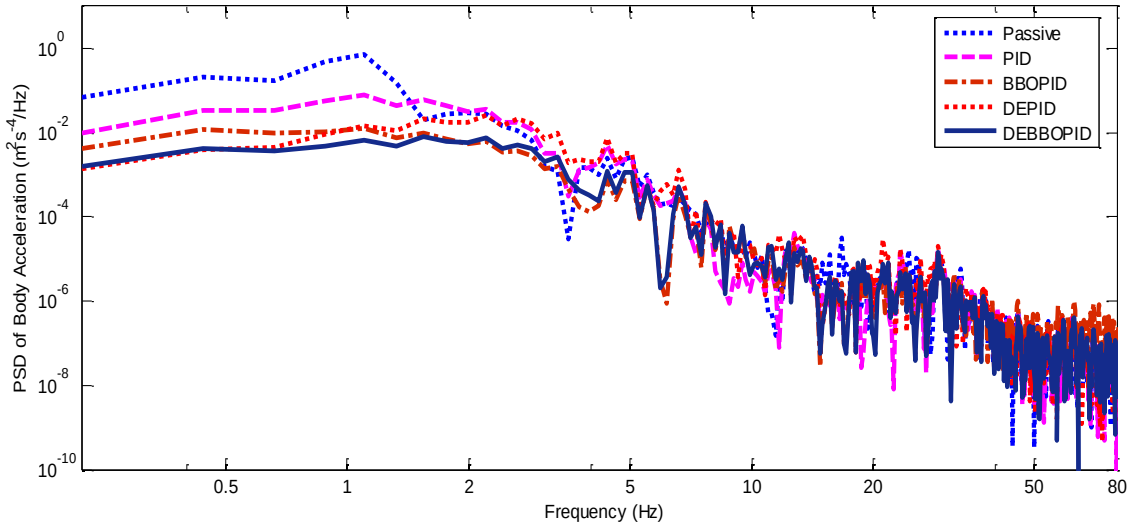

(a)

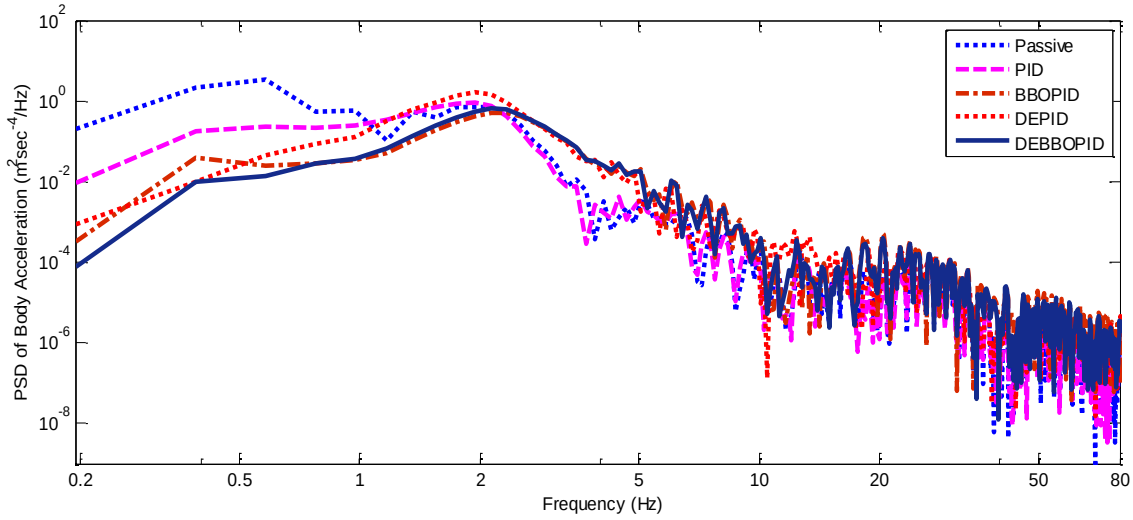

(b)

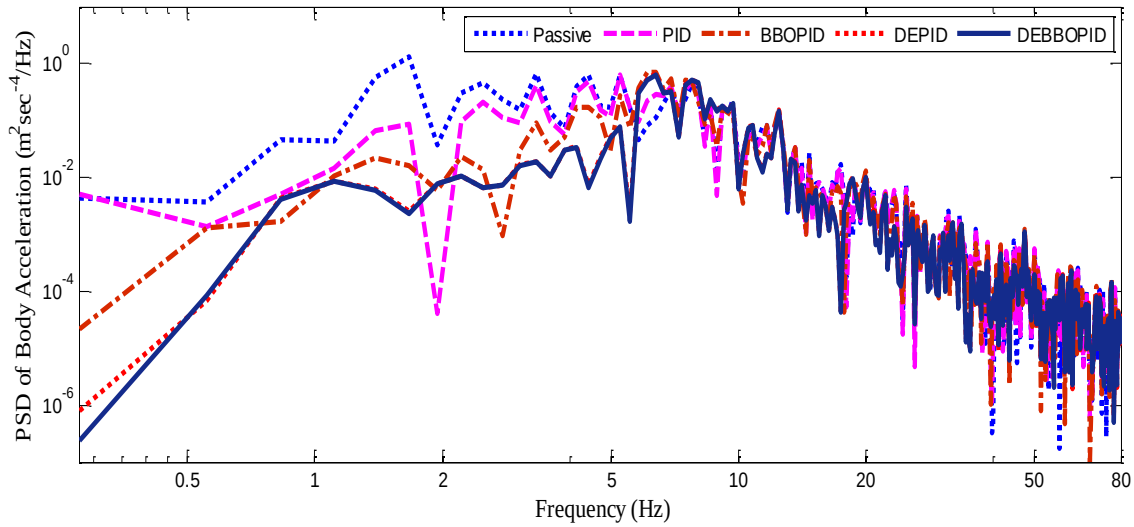

(c)

Figure 9. *PSD* of Body acceleration comparison of Passive, *PID*, *BBOPID*, *DEPID* and *DEBBOPID* with (a) Trapezoidal (b) Step and(c) Random type road inputs in quarter car model

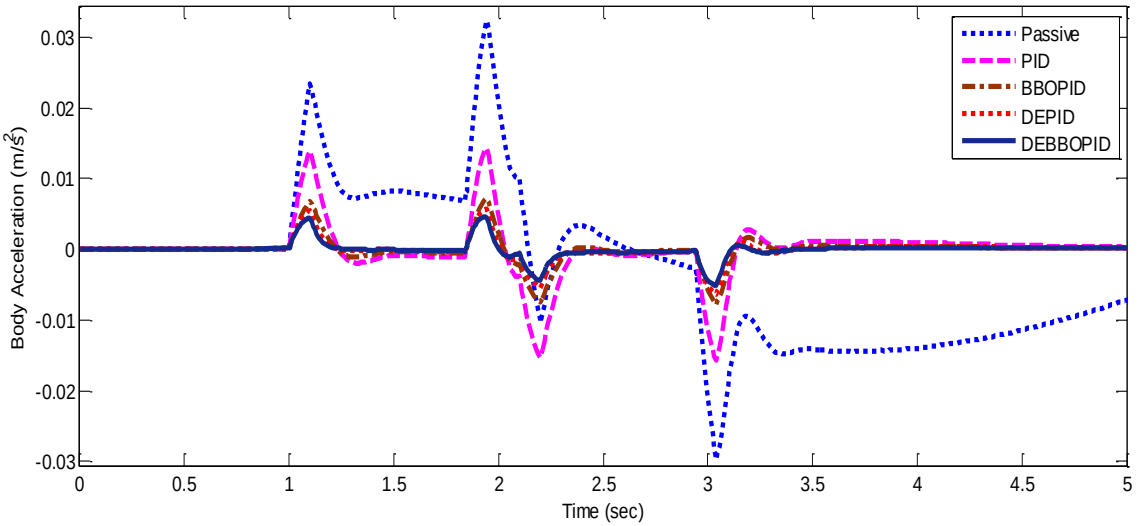

(a)

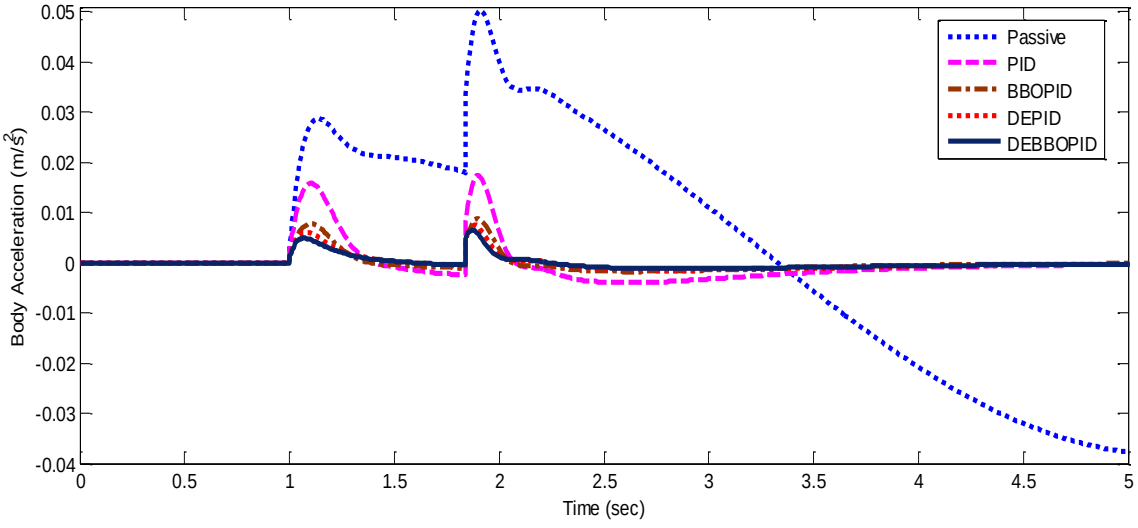

(b)

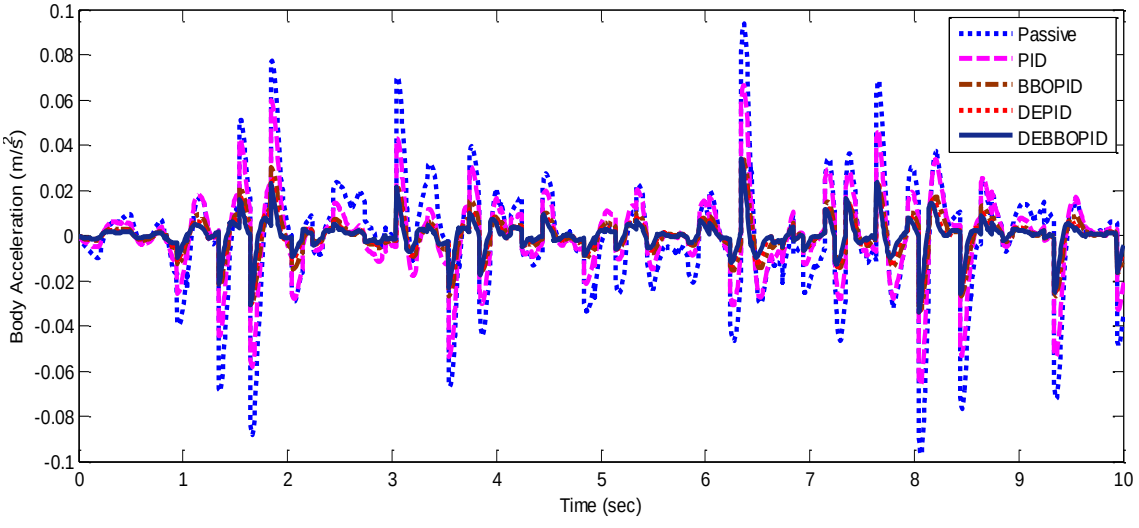

(c)

Figure 10. Body acceleration of half car model with (a) Trapezoidal input (b) Step input and (c) Random input

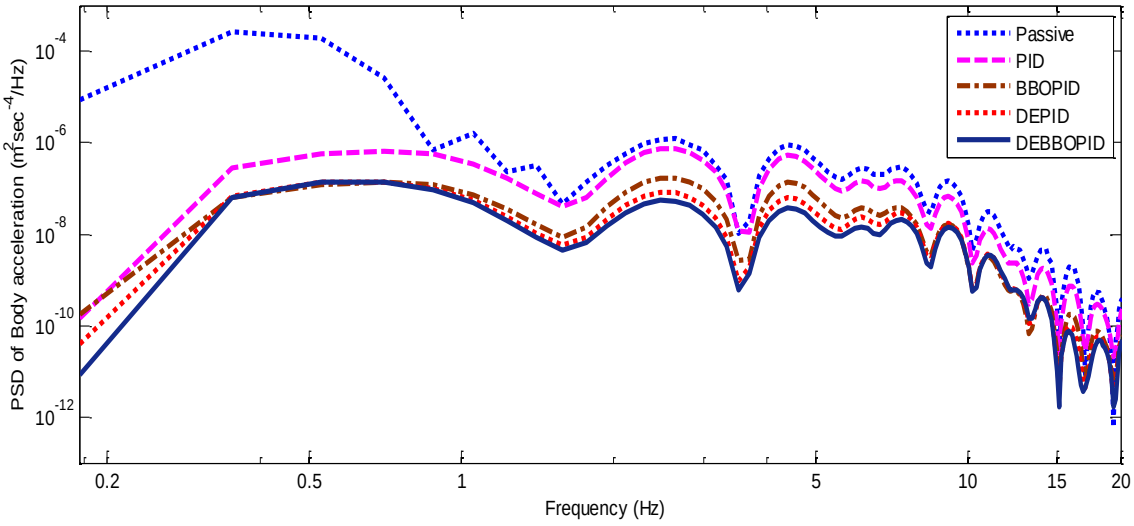

(a)

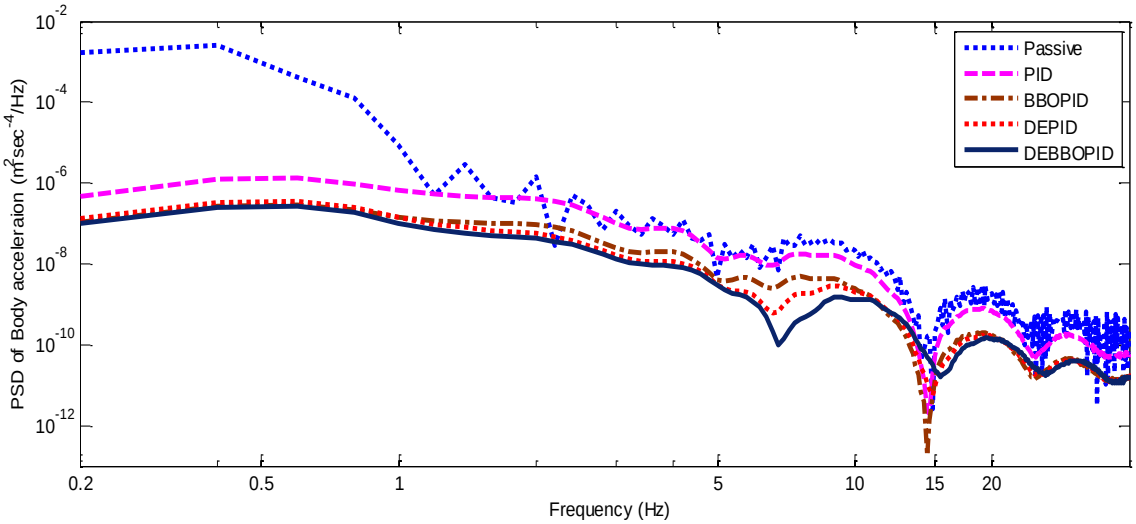

(b)

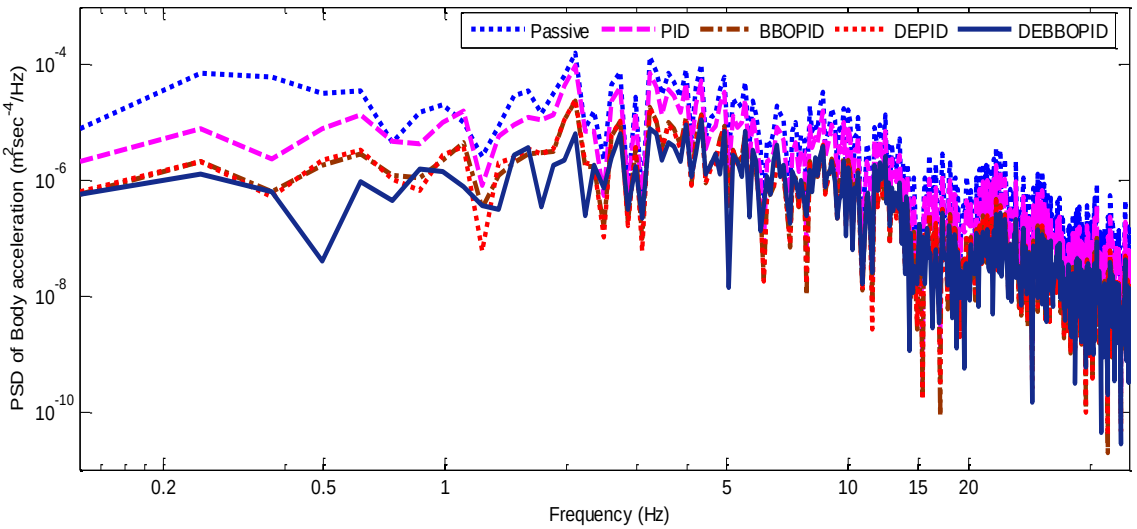

(c)

Figure 11. PSD of Body acceleration comparison of Passive, *PID, BBOPID, DEPID* and *DEBBOPID* with (a) Trapezoidal(b) Step and (c) Random type road inputs in half car model

Table 5. RMS values of the body acceleration of half car model

System	Body Acceleration ($x10^{-6}m/s^2$)		
	Trapezoidal Input	Step input	Random input
Passive	732.92	1289.31	2935.34
PID	366.67	842.25	2423.57
BBOPID	178.41	524.69	2192.04
DEPID	167.49	492.18	1839.65
DEBBOPID	142.03	448.83	1643.97

The results of the HC passive system, system with PID, BBOPID, DEPID and DEBBOPID controllers simulation are shown in Figures 10 and 11. (a) - (c). Also, the RMS values of the body acceleration of the system for different inputs are tabulated in Table 5, which highlights the effectiveness with the DEBBOPID.

5. Conclusions

The optimization of *PID* tuning parameters for the application in *VASS* with linear actuator are discussed in the present paper. Among the three optimization techniques discussed, the *DEBBO* gives a better convergence performance. The *DEBBOPID* results are good compared to the passive system, conventional *PID* controller and *BBOPID* based *VASS*. The *DEBBOPID* reduces the body acceleration considerably and ensures a travelling comfort to the passengers. The controllers, discussed in section 3, are easy to implement and with reference to the *PSD* of body acceleration, it is clear that all the controllers provide a better vibration control compared to the passive system. The *DEBBOPID* gives a better *PSD* and is the best as it converges quickly among the discussed controllers for the control of the vibration in the vehicle.

References

[1] Seok_il Son. Fuzzy logic controller for an automotive active suspension system. Master's Thesis. Syracuse University; 1996.

[2] D. Hrovat, "Survey of advanced suspension developments and related optimal control applications". Automatica, Vol. 33 (1997), 171-181.

[3] D. Hrovart, "Applications of optimal control to dynamic advanced automotive suspension design". ASME Journal of Dynamic Systems, Measurement and Control, (Special issue commemorating 50 years of the DSC division), Vol. 115 (1993), 328-342.

[4] E. Esmailzadeh, H.D. Taghirad, "Active vehicle suspensions with optimal state feedback control". J. Mech. Sci., Vol. 200 (1996), 1-18.

[5] MO. Abdalla, N. Al Shabatat, M. Al Qaisi, "Linear matrix inequality based control of vehicle active suspension system". Vehicle System Dynamics, Vol. 47 (2007), 121-134.

[6] K. Rajeswari, P. Lakshmi, "Vibration control of mechanical suspension system". Int. J. Instrumentation Technology, Vol. 1 (2011), 60-71.

[7] O. Demir, Keskin, S. Cetlin, "Modelling and control of a nonlinear half vehicle suspension system; A hybrid fuzzy logic approach". Nonlinear Dynamics, Vol. 67 (2012), 2139-2151.

[8] C. Yeroglu, N. Tan, "Design of robust PI controller for vehicle suspension system". Journal of Electrical Engineering & Technology, Vol. 3 (2008), 135-142.

[9] Dan Simon, "Biogeography based optimization". IEEE Transactions on Evolutionary Computation, Vol. 12 (2008), 702-713.

[10] V.K. Panchal, Parminder Singh, Navdeep Kaur, Harish Kundra, "Biogeography based satellite image classification". International Journal of Computer Science and Information Security, Vol. 6 (2009), 269-274.

[11] Urvinder Singh, Harish Kumar, Tara Singh Kamal, "Design of Yagi-Uda antenna using biogeography based optimization". IEEE Transactions on Antennas and Propagation, Vol. 58 (2010), 3375- 3379.

[12] Aniruddha Bhattacharya, Pranab Kumar Chattopadhyay, "Biogeography-based optimization for different economic load dispatch problems". IEEE Transactions on Power Systems, Vol. 25 (2010), 1064-1077.

[13] Dan Simon, "A dynamic system model of biogeography-based optimization". Applied Soft Computing, Vol. 11 (2011), 5652–5661.

[14] Abhishek Sinha, Swagatam Das, B. K. Panigrahi, "A linear state-space analysis of the migration model in an island biogeography system". IEEE Transactions on Systems, Man, and Cybernetics—Part A: Systems and Humans, Vol. 41 (2011), 331-337.

[15] K. Jamuna, K.S. Swarup, "Multi-objective biogeography based optimization for optimal PMU placement". Applied Soft Computing, Vol. 12 (2012), 1503-1510.

[16] Aniruddha Bhattacharya, Pranab Kumar Chattopadhyay, "Closure to discussion of "hybrid differential evolution with biogeography-based optimization for solution of economic load dispatch"". IEEE Transactions on Power Systems, Vol. 27 (2012), 575.

[17] Haiping Maa, Dan Simon, Minrui Fei, Zhikun Xie, "Variations of biogeography-based optimization and Markov analysis". Information Sciences, Vol. 220 (2013), 492–506.

[18] M. R. Lohokare, S. S. Pattnaik, B. K. Panigrahi, Sanjoy Das, "Accelerated biogeography based optimization with neighborhood search for optimization". Applied Soft Computing, In press, Unpublished, available on line (2013).

[19] Ilhem Boussaïd, Amitava Chatterjee, Patrick Siarry, Mohamed Ahmed-Nacer, "Hybridizing biogeography-based optimization with differential evolution for optimal power allocation in wireless sensor networks", IEEE Transactions on Vehicular Technology, Vol. 60 (2011), 2347-2353.

[20] K. Rajeswari, P. Lakshmi, "Simulation of suspension system with intelligent active force control". International Conference on Advances in Recent Technologies in Communication and Computing, Chennai, India, 2010.

[21] Yahaya Md. Sam, Johari Halim Shah Bin Osman, "Modeling and control of the active suspension system using proportional integral sliding mode approach". Asian Journal of Control, Vol. 7 (2005), 91-98.

[22] L.C. Saikia, S.K. Das, P. Dash, M. Raju, "Multi — Area AGC with AC/DC link and BES and Cuckoo Search optimized PID controller". 3rd International Conference on Computer, Communication, Control and Information Technology, Hooghly, India, 2015.

[23] T. A. Boghdady, M. M. Sayed, A. M. Emam, E. E. Abu El-Zahab, "A Novel Technique for PID Tuning by Linearized Biogeography-Based Optimization". IEEE 17th International Conference on Computational Science and Engineering, Chengdu, China, 2014.

[24] R. Storn, K. Price, "Differential evolution - a simple and efficient heuristic for global optimization over continuous

spaces". Journal of Global Optimization, Vol. 11 (1997), 341-359.

[25] Rukmini V Kasarapu, Vijaya B. Vommi, "Economic design of joint *X* and R control charts using differential evolution". Jordan Journal of Mechanical and Industrial Engineering, Vol. 5, (2011) No. 2, 149-160.

[26] Aniruddha Bhattacharya, P.K. Chattopadhyay, "Hybrid differential evolution with biogeography-based optimization algorithm for solution of economic emission load dispatch problems". Expert Systems with Applications, Vol. 38 (2011), 14001–14010.

[27] R. Kalaivani, P. Lakshmi, K. Sudhagar, "Hybrid (DEBBO) Fuzzy Logic Controller for quarter car model: DEBBOFLC for Quarter Car model". UKACC International Conference on Control (CONTROL), Loughborough, U.K., 2014.